

# Structural, Vibrational, and Electronic Study of Sb<sub>2</sub>S<sub>3</sub> at High Pressure

J. Ibáñez,<sup>†</sup> J.A. Sans,<sup>‡</sup> C. Popescu,<sup>§</sup> J. López-Vidrier,<sup>†</sup> J.J. Elvira-Betanzos,<sup>†</sup>  
V.P. Cuenca-Gotor,<sup>‡</sup> O.Gomis,<sup>°</sup> F.J. Manjón,<sup>\*,‡</sup> P. Rodríguez-Hernández,<sup>‡</sup> and A.  
Muñoz<sup>‡</sup>

<sup>†</sup> Institute of Earth Sciences Jaume Almera, CSIC, 08028 Barcelona, Spain

<sup>‡</sup> Instituto de Diseño para la Fabricación y Producción Automatizada, MALTA Consolider Team,  
Universitat Politècnica de València, 46022 València, Spain,

<sup>§</sup> ALBA-CELLS, 08290 Cerdanyola del Vallès, Barcelona, Spain

<sup>°</sup> Centro de Tecnologías Físicas: Acústica, Materiales y Astrofísica, MALTA Consolider Team,  
Universitat Politècnica de València, València, Spain

<sup>‡</sup> Departamento de Física, Instituto de Materiales y Nanotecnología, MALTA Consolider Team,  
Universidad de La Laguna, 38207 San Cristobal de la Laguna, Tenerife, Spain

## Corresponding Author

\*E-mail: fjmanjon@fis.upv.es. Telephone: (+34) 963877000 ext (75287).

## Supporting Information

### S.1. Vibrational properties of Sb<sub>2</sub>S<sub>3</sub>

In order to understand the lattice dynamics of Sb<sub>2</sub>S<sub>3</sub> it is important to remind that the structure of Sb<sub>2</sub>S<sub>3</sub> is composed of linked SbS<sub>3</sub>E and SbS<sub>5</sub>E units, here E refers to the lone electron pair of Sb atoms, since the vibrational modes of chalcogenide compounds have been usually interpreted in a simplified manner in terms of molecular-like units. Within this context, the optical phonons of Sb<sub>2</sub>S<sub>3</sub> have been partially interpreted in the past as coming solely from SbS<sub>3</sub> units (without any mention to SbS<sub>5</sub> units) [1,2]. The undistorted SbS<sub>3</sub> units, which have an ideal trigonal pyramidal (C<sub>3v</sub>) symmetry, give rise to four normal modes of vibration: symmetric stretching  $\nu_1(A_1)$ , anti-symmetric stretching  $\nu_3(E)$ , symmetric bending  $\nu_2(A_1)$ , and anti-symmetric bending  $\nu_4(E)$ . Koudelka *et al.* estimated the frequencies of SbS<sub>3</sub> units from those measured in SbCl<sub>3</sub> molecules and found them to be close to 112, 138, 269, and 302 cm<sup>-1</sup> [1]. Following similar arguments, the undistorted SbS<sub>5</sub> units, which have an ideal tetragonal pyramidal (C<sub>4v</sub>) symmetry, give rise to nine normal modes of vibration: axial stretching  $\nu_1(A_1)$ , antisymmetric in-plane stretching  $\nu_4(B_1)$ , antisymmetric in-plane stretching+bending

$\nu_7(E)$ , symmetric in-plane stretching  $\nu_2(A_1)$ , antisymmetric in-plane bending  $\nu_8(E)$ , symmetric in-plane bending  $\nu_3(A_1)$ , anti-symmetric out-of-plane bending  $\nu_5(B_1)$ , anti-symmetric in-plane bending  $\nu_6(B_2)$  and symmetric in-plane bending  $\nu_9(E)$ . Stretching modes in distorted tetragonal pyramidal  $SbS_5$  units (similar to those of stibnite) can be observed for instance in  $MnSb_2S_4$ , with frequency values around 283 and 300  $cm^{-1}$  [3]. Despite pure vibrations of  $SbS_3$  units should display considerable higher frequencies (340-380  $cm^{-1}$ ) than those observed in  $Sb(SR)_3$  molecules [4,5], the vibrational frequencies of  $MnSb_2S_4$  have been previously interpreted as due to  $SbS_3$  units instead of distorted  $SbS_5$  units. These arguments suggest that stretching frequencies around 300  $cm^{-1}$  in undistorted  $SbS_5$  units and above 340  $cm^{-1}$  in undistorted  $SbS_3$  units would be expected, which are consistent with the shorter average Sb-S bond distances in  $SbS_3$  units as compared to the  $SbS_5$  units.

To finish this section and just to give an insight of the complex lattice dynamics of  $Sb_2S_3$ , we can mention that both  $SbS_3$  and  $SbS_5$  units are linked in stibnite so they have smaller symmetry than in the ideal configuration. This decrease in symmetry leads to splitting of the doubly degenerated E modes of the isolated units. Furthermore, normal vibrations corresponding to  $SbS_3$  and  $SbS_5$  units get mixed in  $Sb_2S_3$ , which makes difficult the assignment of the Raman modes. In particular, the link of  $SbS_3$  units with neighboring  $SbS_3$  and  $SbS_5$  units makes impossible the observation of pure symmetric and anti-symmetric stretching modes of  $SbS_3$  units in  $Sb_2S_3$ . According to our calculations, the optical mode with the lowest frequency is a silent mode of  $A_u$  symmetry with theoretical frequency near 25  $cm^{-1}$  at room pressure. This mode corresponds to the typical shear mode between alternate layers of layered materials. On the contrary, the two highest optical modes are infrared-active modes of  $B_{1u}$  and  $B_{3u}$  symmetry corresponding to the mixture of a partial symmetric stretching  $\nu_1(A_1)$  of  $SbS_3$  units and axial stretching  $\nu_1(A_1)$  of  $SbS_5$  units. In fact, the highest Raman active modes are two pairs of  $(A_g + B_{2g})$  modes, which correspond to partial anti-symmetric  $\nu_3$  stretching of  $SbS_3$  units and  $\nu_8$  stretching of  $SbS_5$  units together with partial  $\nu_2$  bending of  $SbS_3$  units and  $\nu_1$  stretching of  $SbS_5$  units, respectively. This mixture of stretching or stretching and bending modes of  $SbS_3$  and  $SbS_5$  units allows us to explain why the maximum frequency of Raman-active modes in  $Sb_2S_3$  is slightly above 300  $cm^{-1}$  and well below 340  $cm^{-1}$ .

## S.2. Calculated lattice parameters and atomic coordinates of Bi<sub>2</sub>S<sub>3</sub> and Sb<sub>2</sub>Se<sub>3</sub>.

**Table S1.** Experimental (exptl) and theoretical (theor) values of atomic positions of Bi<sub>2</sub>S<sub>3</sub> at room pressure. Experimental and theoretical lattice parameters are: experiment:  $a = 11.269(2)$ ,  $b = 3.9717(3)$  Å,  $c = 11.129(2)$  Å (from **Ref. 6**), theory:  $a = 11.40958$  Å,  $b = 3.9680$  Å and  $c = 11.0068$  Å.

Atom	x	y	z
Bi(1)	0.0164(2) (exptl)	0.25 (exptl)	0.6745(2) (exptl)
	0.0149 (theor)	0.25 (theor)	0.6750 (theor)
Bi(2)	0.3406(3) (exptl)	0.25 (exptl)	0.4661(2) (exptl)
	0.3608 (theor)	0.25 (theor)	0.4638 (theor)
S(1)	0.0494(16) (exptl)	0.25 (exptl)	0.1311(11) (exptl)
	0.0476 (theor)	0.25 (theor)	0.1294 (theor)
S(2)	0.3773(17) (exptl)	0.25 (exptl)	0.0604(12) (exptl)
	0.3768 (theor)	0.25 (theor)	0.0554 (theor)
S(3)	0.2165(16) (exptl)	0.25 (exptl)	0.8069(12) (exptl)
	0.2142 (theor)	0.25 (theor)	0.8080 (theor)

**Table S2.** Experimental (exptl) and theoretical (theor) values of atomic positions of Sb<sub>2</sub>Se<sub>3</sub> at room pressure. Experimental and theoretical lattice parameters are: experiment:  $a = 11.80$ ,  $b = 3.97$  Å and  $c = 11.65$  Å (from **Ref. 7**), theory:  $a = 11.7968$  Å,  $b = 3.9818$  Å and  $c = 11.2831$  Å.

Atom	x	y	z
Sb(1)	0.4971(1) (exptl)	0.25 (exptl)	0.8228(3) (exptl)
	0.5226 (theor)	0.25 (theor)	0.8290 (theor)
Sb(2)	0.3432(1) (exptl)	0.25 (exptl)	0.4559(2) (exptl)
	0.3499 (theor)	0.25 (theor)	0.4624 (theor)
Se(1)	0.7162(2) (exptl)	0.25 (exptl)	0.7105(3) (exptl)
	0.7149 (theor)	0.25 (theor)	0.6966 (theor)
Se(2)	0.5597(3) (exptl)	0.25 (exptl)	0.3673(2) (exptl)
	0.5536 (theor)	0.25 (theor)	0.3667 (theor)
Se(3)	0.3675(2) (exptl)	0.25 (exptl)	0.0629(3) (exptl)
	0.3706 (theor)	0.25 (theor)	0.0521 (theor)

### S.3. Pressure dependence of bond-lengths in $\text{Bi}_2\text{S}_3$ and $\text{Sb}_2\text{Se}_3$ .

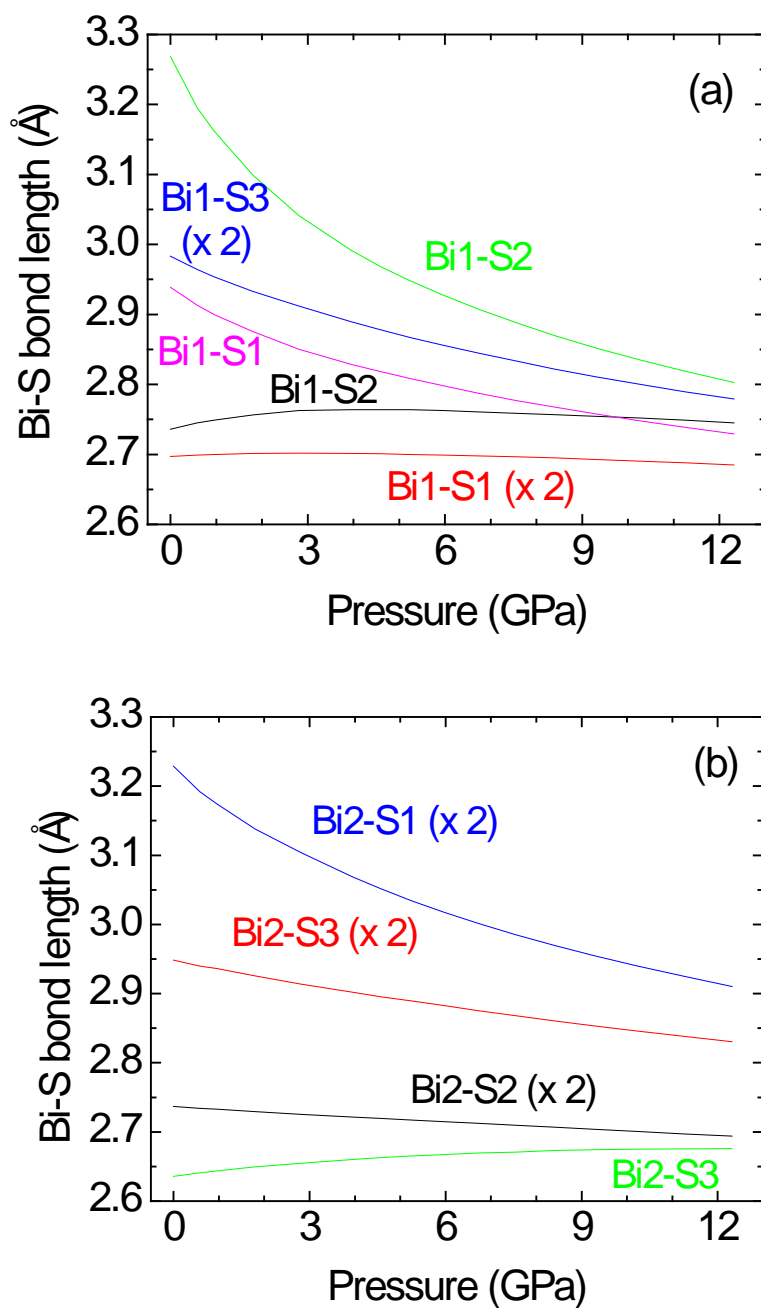


**Fig. S1** (a) Theoretical pressure dependence of the Bi(1)-S bond lengths in  $\text{Bi}_2\text{S}_3$ . (b) Idem for the Bi(2)-S bond lengths.

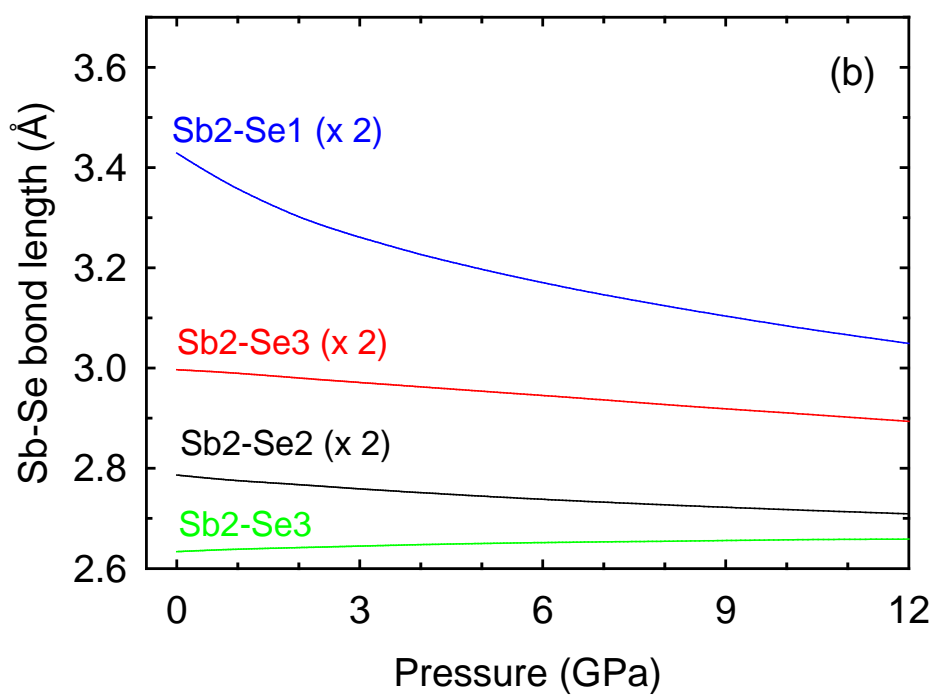
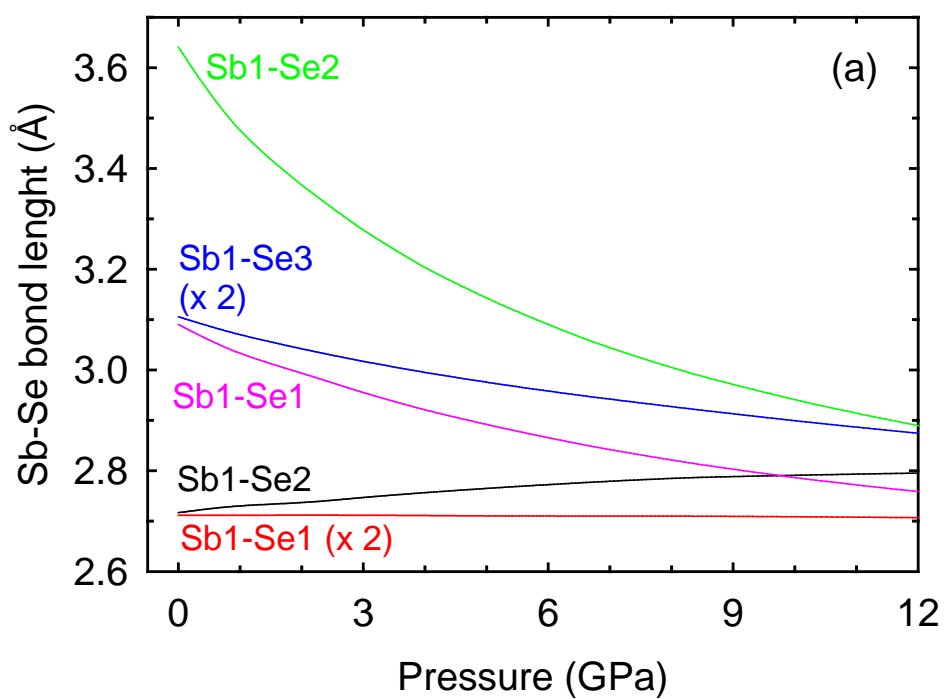


**Fig. S2** (a) Theoretical pressure dependence of the Sb(1)-Se bond lengths in  $\text{Sb}_2\text{Se}_3$ . (b) Idem for the Sb(2)-Se bond lengths.

#### S.4. Pressure dependence of Raman-active modes in $\text{Bi}_2\text{S}_3$ and $\text{Sb}_2\text{Se}_3$ .

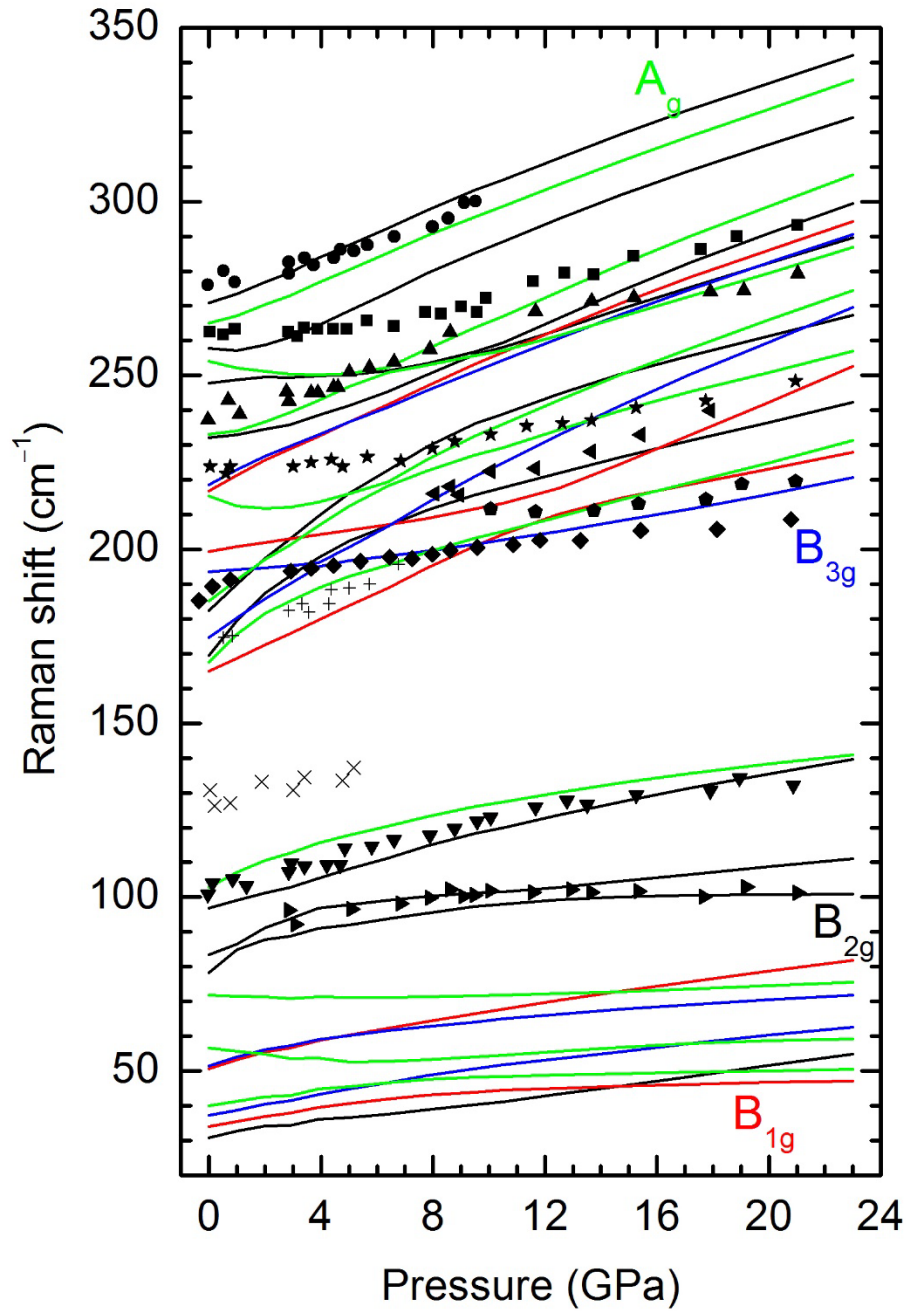


**Fig. S3** Experimental (symbols) and theoretical (lines) pressure dependence of the Raman-mode frequencies of  $\text{Bi}_2\text{S}_3$ . Different colors represent Raman-active modes of different symmetries.

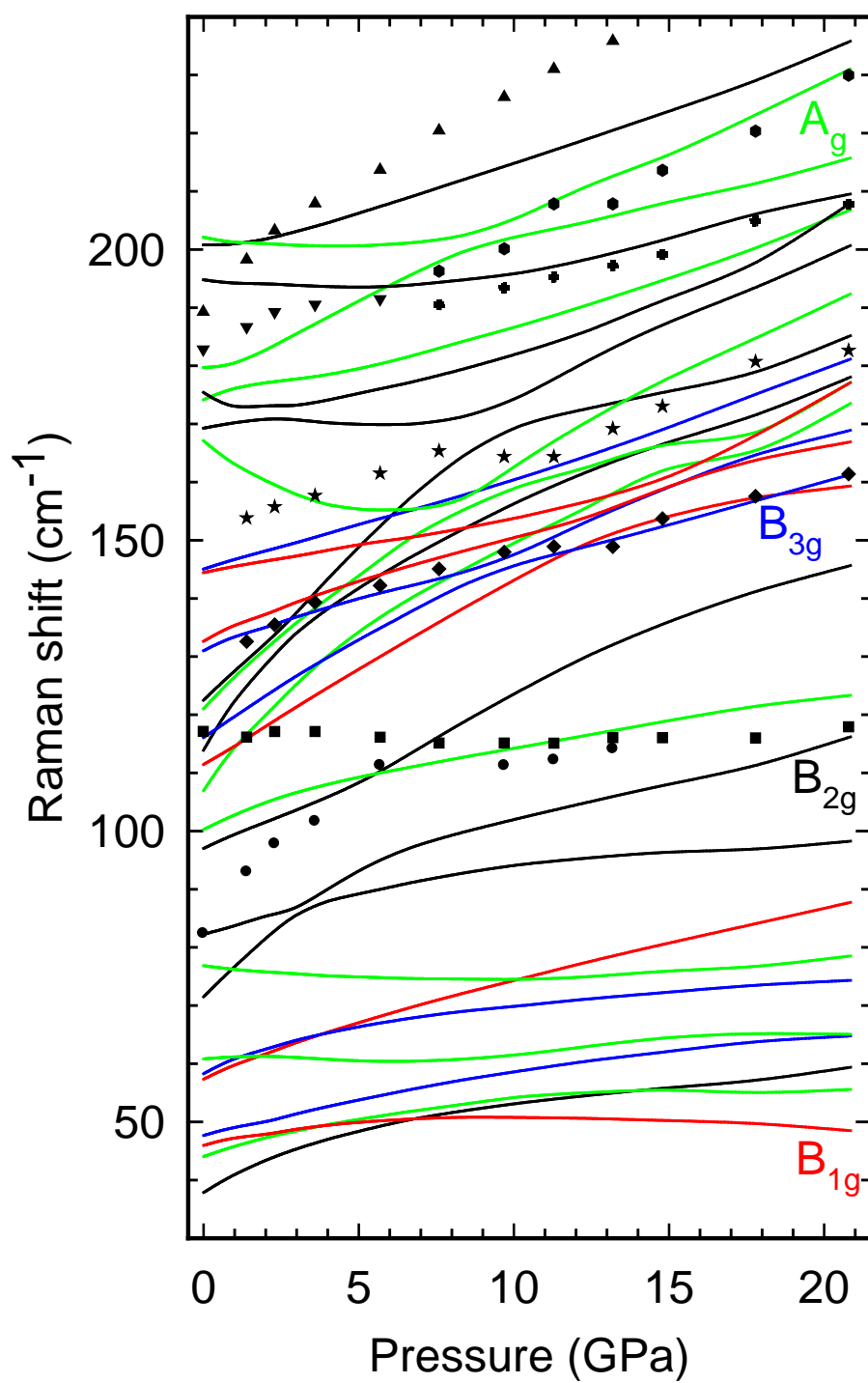


**Fig. S4** Experimental (symbols) and theoretical (lines) pressure dependence of the Raman-mode frequencies of  $\text{Sb}_2\text{Se}_3$ . Different colors represent Raman-active modes of different symmetries.

**S.5. Pressure dependence of electronic band structure in  $\text{Bi}_2\text{S}_3$  and  $\text{Sb}_2\text{Se}_3$ .**

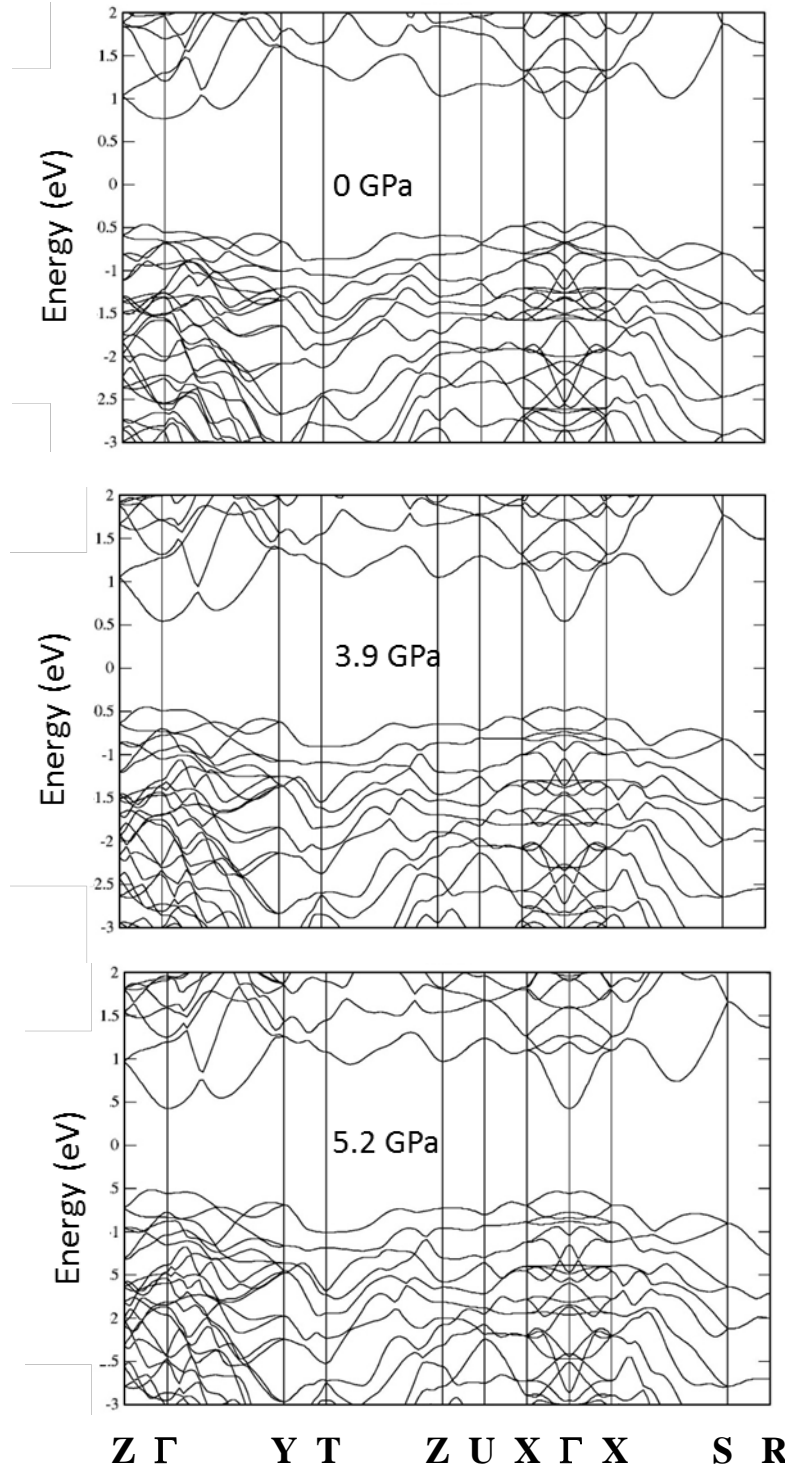


**Fig. S5** Calculated electronic band structure of  $\text{Bi}_2\text{S}_3$  at 0, 3.9 and 5.2 GPa.



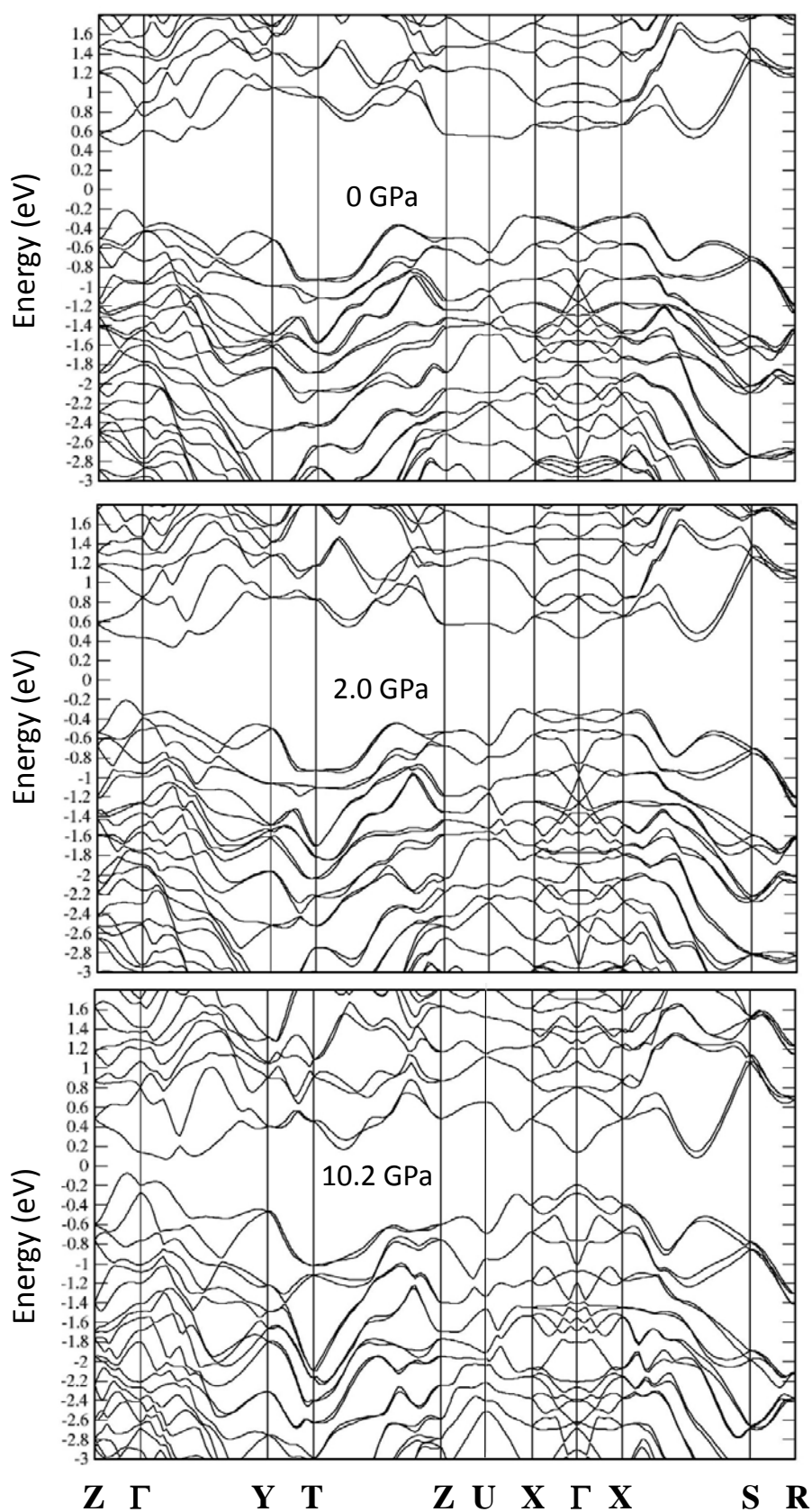


**Fig. S6** Calculated electronic band structure of  $\text{Sb}_2\text{Se}_3$  at 0, 2.0, and 10.2 GPa.

## Bibliography

- [1] Koudelka, L.; Horak, J.; Pisarcik, M. Raman Spectra of the  $(\text{GeS}_2)_{1-x}(\text{Sb}_2\text{S}_3)_x$  System. *Chem. Zvesti* **1981**, 35, 327-332.
- [2] Kharbish, S.; Libowitzky, E.; Beran, A. Raman Spectra of Isolated and Interconnected Pyramidal  $\text{XS}_3$  Groups ( $\text{X} = \text{Sb}, \text{Bi}$ ) in Stibnite, Bismuthinite, Kermesite, Stephanite and Bournonite. *Eur. J. Mineral.* **2009**, 21, 325-333.
- [3] Pfizner A.; Kurowski, D. A New Modification of  $\text{MnSb}_2\text{S}_4$  Crystallizing in the  $\text{HgBi}_2\text{S}_4$  Structure Type. *Z. Kristall.* **2009**, 215, 373-376.
- [4] Pfizner, A. Copper Iodide as Solid Solvent for Thiometalate Ions. *Chem. Eur. J.* **1997**, 3, 2032-2038.
- [5] Weidlein, J.; Müller, U.; Dehnicke, K.; Schwingungsfrequenzen I. Thieme, Stuttgart, **1981**, p. 155.
- [6] Lundegaard, L. F.; Makovicky, E.; Boffa-Ballaran, T.; Balic-Zunic, T. Crystal Structure and Cation Lone Electron Pair Activity of  $\text{Bi}_2\text{S}_3$  between 0 and 10 GPa. *Phys. Chem. Minerals* **2005**, 32, 578-584.
- [7] Efthimiopoulos, I.; Zhang, J.M.; Kucway, M.; Park, C. Y.; Ewing, R.C.; Wang, Y.  $\text{Sb}_2\text{Se}_3$  Under Pressure. *Sci. Rep.* **2013**, 3, 2665-2672.